



FULL PAPER

A copper diimine-based honeycomb-like porous network as an efficient reduction catalyst

Abrar Ahmad¹ | Syed Niaz Ali Shah¹ | Mehwish Arshad¹ |
Francine Bélanger-Gariepy² | Edward R.T. Tiekink³ | Zia ur Rehman¹

¹Department of Chemistry, Quaid-i-Azam University, Islamabad, 45320, Pakistan

²Department of Chemistry, University of Montreal, Montreal, Quebec, H3T 1J4, Canada

³Research Centre for Crystalline Materials, School of Science and Technology, Sunway University, Subang Jay, 47500, Malaysia

Correspondence

Zia ur Rehman, Department of Chemistry, Quaid-i-Azam University, Islamabad 45320, Pakistan.
Email: zrehman@qau.edu.pk; hafizqau@yahoo.com

Funding information

Higher Education Commission of Pakistan

Nitrophenols are among the widely used industrial chemicals worldwide; however, their hazardous effects on environment are a major concern nowadays. Therefore, the conversion of environmentally detrimental *p*-nitrophenol (PNP) to industrially valuable *p*-aminophenol (PAP), a prototype reaction, is an important organic transformation reaction. However, the traditional conversion of PNP to PAP is an expensive and environmentally unfriendly process. Here, we report a honeycomb-like porous network with zeolite-like channels formed by the self-organization of copper, 1,10-phenanthroline, 4,4'-bipyridine, and water. This porous network effectively catalyzed the transformation of hazardous PNP to pharmaceutically valued PAP. In the presence of complex, PNP to PAP conversion occurred in a few minutes, which is otherwise a very sluggish process. To assess the kinetics, the catalytic conversion of PNP to PAP was studied at five different temperatures. The linearity of $\ln C_t/C_0$ versus temperature plot indicated pseudo-first-order kinetics. The copper complex with zeolite like channels may find applications as a reduction catalyst both on laboratory and industrial scales and in green chemistry for the remediation of pollutants.

KEYWORDS

catalyst, copper complex, porous network, zeolite-like channels

1 | INTRODUCTION

Nitrophenols are among the most widely used industrial chemicals worldwide because of their applications in explosives, pesticides, dyes, and rubber materials.^[1] However, owing to their carcinogenic and hazardous nature, the US Environmental Protection Agency (EPA) has enlisted them among the top organic pollutants.^[2] Once internalized in the bloodstream, nitrophenols can cause a variety of problems including methemoglobinemia, decrease ATP production, damage lungs, and affect the nervous system, dermatitis, hormonal disorders, renal failure, skin damages, and eyes irritations.^[3]

To remove this stable, water-soluble, and environmentally hazardous^[4] material, several strategies have

been employed, including adsorption,^[5] microbial degradation,^[6] photocatalytic degradation,^[7] the electro-Fenton method,^[8] electrocoagulation,^[9] and electrochemical treatment.^[10] The conversion of environmentally detrimental *p*-nitrophenol (PNP) to industrially valuable *p*-aminophenol (PAP) is a very important organic transformation reaction. The latter is used in various antipyretic and analgesic drugs such as paracetamol, corrosion inhibitor, lubricant, and dyeing agent.^[11] However, the traditional conversion of PNP to PAP is carried out in organic solvent under high pressure making this an expensive and environmentally unfriendly process.^[12]

To ensure the foregoing conversion in an inexpensive and environmentally friendly manner, a smart strategy is

usually adopted, that is, via a catalytic reduction in aqueous media. In this context, various metal-based nanocatalysts including those of Au,^[12,13] Ag,^[14] Pd,^[15] Cu,^[16] Zn, and Ni^[17] have been used. To further enhance the stability and catalytic efficacy, these materials can be supported on polymers, oxides, resins, TiO₂, SiO₂, and carbon. Furthermore, some of these metals (e.g., Au, Pd, and Pt) are too expensive for practical applications on a large scale. Literature studies reveal that photocatalytic reduction of PNP is mostly carried out by heterogeneous catalysis using various metal-based nanostructures.^[18–20] However, no homogenous catalyst has been reported so far to reduce PNP to PAP.

Sparked by the challenge that coordination chemistry could be exploited to mimic naturally occurring three-dimensional materials,^[21] crystal engineers have responded with a literal plethora of metal-organic framework (MOF) sustained by a combination of covalent/dative bonding interactions between practically all available metals and a huge diversity in ligands.^[22] The opportunities for tuning/fine-tuning synthetic outcomes by combining metal centers, for example, choice of metal, oxidation state, and coordination geometry preference, with ligands, for example, charged or neutral, variable donor atoms, and denticity, are enormous. Conversely, this variety of options coupled with the observation that reaction outcomes are sometimes dependent on the solvent, temperature, concentration of reagents, etc.^[23] means that there is practically an unlimited number of MOFs that can be generated. All this, of course, ignores two-dimensional coordination polymers, the focus of the present report, let alone one-dimensional chains. Links between lower dimensional architectures can be anyone or a combination of noncovalent interactions,^[24] with hydrogen bonding obviously being prominent^[25] but halogen bonding^[26] and interactions involving “metallo-ligands”^[27] also being important.

Recently, copper-based catalysts, owing to their impressive advantages over other transition metal catalysts, have received a significant attention. Their lower cost, readily availability, insensitivity to air, easy handling, and generation of less waste make them versatile catalysts in various organic reaction like synthesis of enzymes,^[28] oxidative polymerization of aniline,^[29] rearrangement reactions of aldoxime,^[30] and reductions of nitroarenes.^[20] Furthermore, copper is the second abundant transition metal inside human body and can be easily metabolized by the body metabolic system.^[31] Its antimicrobial nature and biocompatible features make it a suitable catalyst for biological applications.^[32]

Among the myriad of practical applications of MOF materials, owing to their zeolite-like pores, subsequent high surface area, and stability, relates to their high

catalytic potential,^[21,22] which indeed has inspired a large number of recent reviews on the utility of both transition metal- and lanthanide-based coordination polymers for catalytic applications.^[33] Literature survey shows that the incorporation of PNP and BH₄[−] into the pores of a porous structure has also been observed in case of certain porous zeolites^[34] and MOF-supported photocatalyst.^[35]

During our on-going studies in copper chemistry,^[36] a zero-dimensional copper diimine complex, whereby the dimer is connected into a three-dimensional architecture via conventional hydrogen bonding interactions to generate a honeycomb-like porous network, has been synthesized, characterized, and investigated as a catalyst for PNP reduction to PAN.

2 | MATERIALS AND METHODS

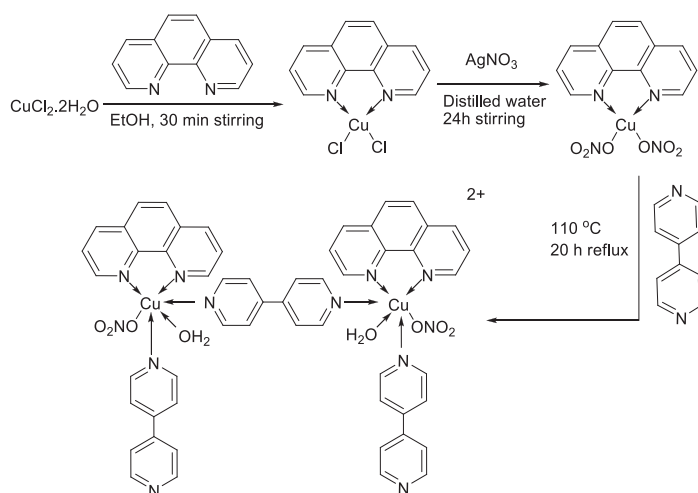
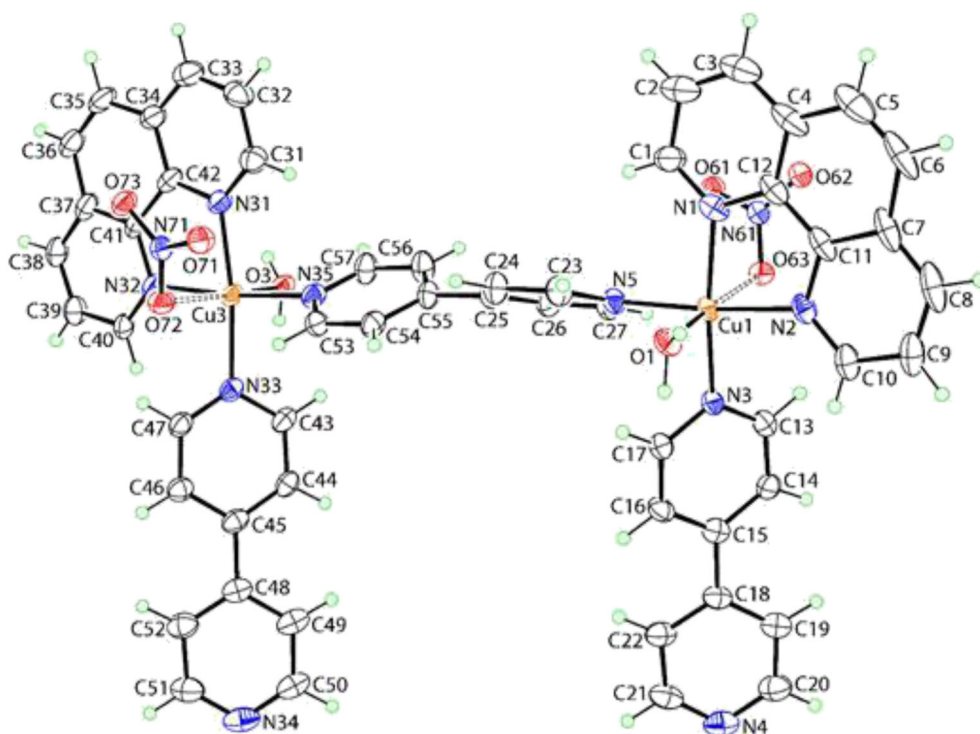
Analytical grade chemicals were purchased from Merck (copper(II) chloride dihydrate), Sigma-Aldrich (1,10-phenanthroline [phen], 4,4'-bipyridine [bipy], sodium borohydride, silver nitrate, and ethanol), and Fluka (PNP) companies.

2.1 | Synthesis of the copper diimine complex

An ethanolic solution (25 mL) of phen (0.58 g, 2.9 mmol) was added dropwise to a CuCl₂·2H₂O (0.50 g, 2.9 mmol) solution (25 mL) in the same solvent, and the mixture was stirred for 30 min at room temperature. The light blue precipitates thus obtained were filtered off and dried in the open air. The precipitates (0.714 g, 2.27 mmol) were re-dissolved in distilled water in a two-necked flask and treated with AgNO₃ (0.77 g, 4.51 mmol) in the dark and stirred for 24 h. To remove AgCl, the solution was filtered, and to this, an ethanolic solution of bipy (0.35 g, 2.27 mmol) was added dropwise followed by reflux at 110°C till the turbidity cleared (Scheme 1). Blue crystals were obtained from the slow evaporation of the final filtered solution. Yield 78% (0.54 g); m.p. 270–272 °C; Fourier transform infrared (FT-IR) (cm^{−1}): 3,441 ν (O–H), 3,040 ν (C–H)aromatic; 1,659 ν (C=N); 1,612 ν (C=C) aromatic; 1,522 ν (ring vibration); 1,494 ν (N–O)_{asym}; 1,305 ν (N–O)_{sym}.

2.2 | Characterization

Gallenkamp (UK) electrothermal melting point apparatus, ultraviolet–visible (UV–vis) spectrophotometer (Model TCC-240A, CAT. No. 204-05557) Shimadzu 1800

SCHEME 1 Synthesis of homobimetallic copper complex, **1****FIGURE 1** Molecular structure of the binuclear copper complex, **1**

double beam (Japan) and Perkin Elmer Spectrum 1000 (USA) instruments were used for recording melting

point, time-dependent UV-vis and FT-IR spectra, respectively.

TABLE 1 Selected bond lengths (Å) for **1**

Parameters	Cu1	Cu3
Cu–N (bridging bipy)	2.009(3)	1.995(3)
Cu–N (terminal bipy)	2.010(3)	2.019(3)
Cu–N (phen, trans to terminal bipy)	2.018(3)	2.015(3)
Cu–N (phen, trans to bridging bipy)	2.024(3)	2.037(3)
Cu–O (aqua)	2.265(3)	2.280(3)
Cu–O (nitrate)	2.745(3)	2.718(3)

Abbreviation: bipy, 4,4'-bipyridine.

2.3 | Single crystal study

Intensity data for a blue block (0.08 × 0.20 × 30 mm) were measured at 100 K on a Bruker Venture Metal jet diffractometer using Ga K α radiation ($\lambda = 1.34139$ Å) so that $2\theta_{\max} = 54.9^\circ$. A total of 69,840 absorption-corrected^[37] data were collected of which 11,307 were unique ($R_{\text{int}} = 0.051$), and of these, 9,908 satisfied the $I \geq 2\sigma(I)$ criterion. The structure was solved by SHELXT^[38] and refined on F^2 with SHELXL-2014/7^[39]

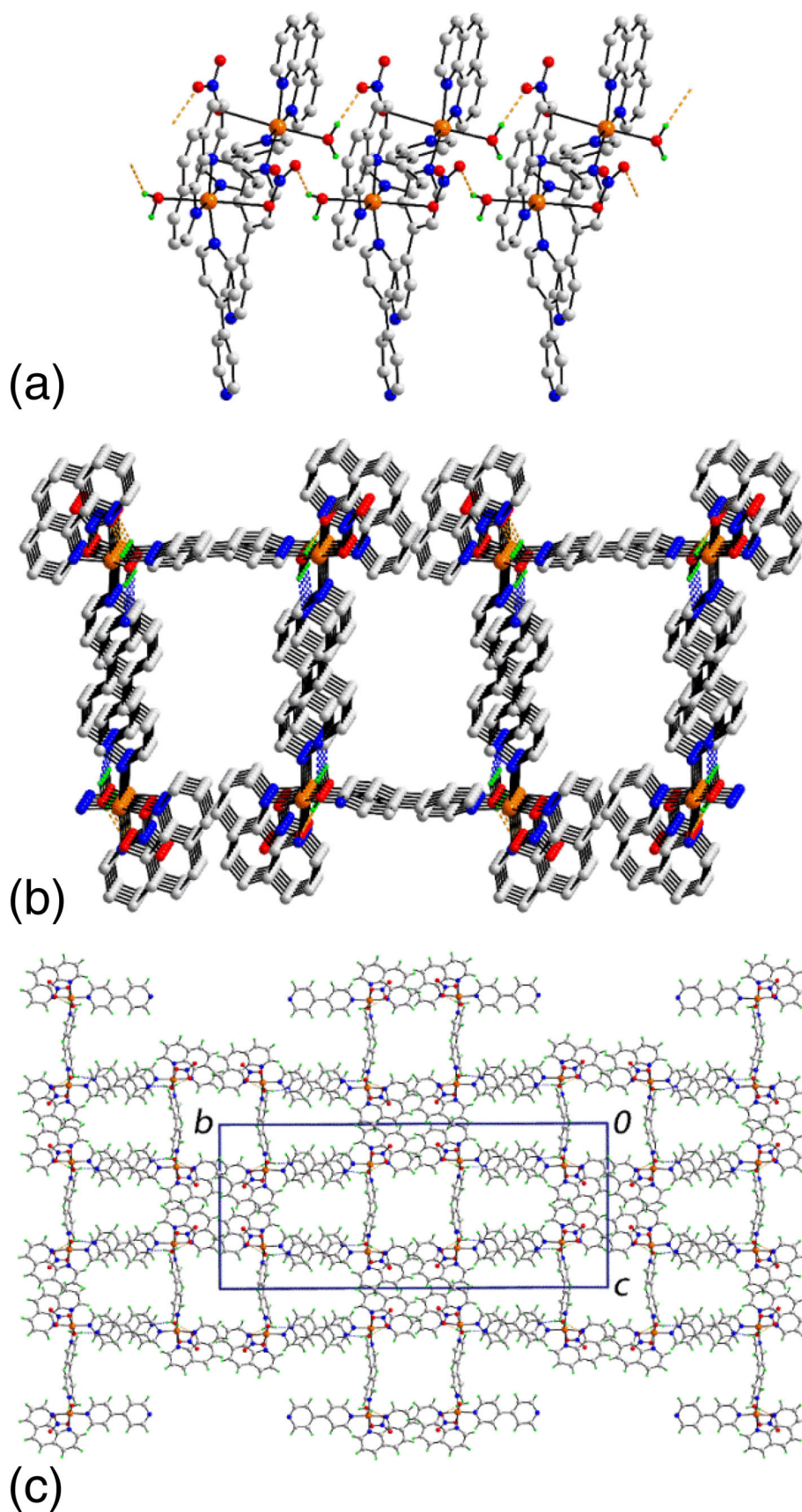


FIGURE 2 Molecular packing for **1**: (a) a view of the supramolecular chain along the a -axis mediated by aqua-O—H \cdots O (nitrate) hydrogen bonding, shown as orange dashed lines, (b) a view of the supramolecular layer in the ac -plane with aqua-O—H \cdots N (pyridyl) hydrogen bonds shown as blue dashed lines (nonparticipating H atoms have been omitted), and (c) a view in projection down the a -axis of the unit cell contents highlighting the channels parallel to the a -axis

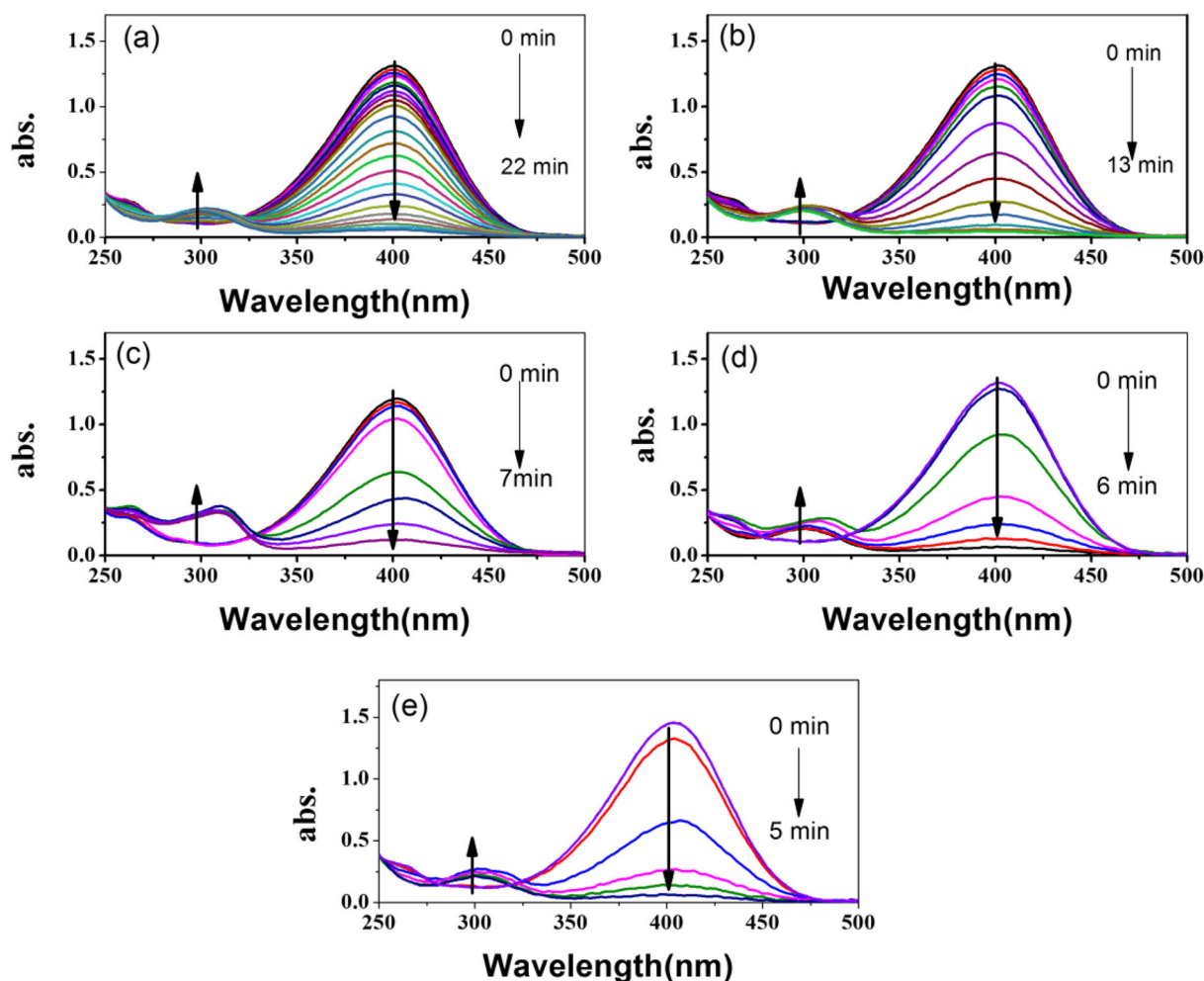


FIGURE 3 Time-dependent ultraviolet-visible (UV-vis) spectra for the reduction of *p*-nitrophenol (PNP) to *p*-aminophenol (PAP) at five different temperatures: (a) 25°C, (b) 30°C, (c) 35°C, (d) 40°C, and (e) 45°C

integrated within Olex.^[40] Nonhydrogen atoms were refined anisotropically, and nonacidic H atoms were included in the model in their calculated positions. The water-H atoms were located and refined without restraint. At this stage of the refinement, the presence of heavily disordered solvent molecules, that is, ethanol and water, were indicated. These were modeled employing the SQUEEZE routine^[41] with full details given in the deposited CIF. The final refinement (701 parameters) had a weighting scheme of the form $w = 1/[s2(F_o^2) + 0.052P2 + 13.335P]$ where $P = (F_o^2 + 2F_c^2)/3$ on F^2 and converged with $R = 0.065$ and $wR^2 = 0.171$. The molecular structure diagram was generated with ORTEP for Windows^[42] at the 35% probability level, and the packing diagrams were drawn with DIAMOND.^[43]

Crystal data for $C_{54}H_{44}Cu_2N_{12}O_8$ (**1**); exclusive of unresolved solvent) $M = 1,116.09$, monoclinic space group $P2_1/c$, $a = 7.3006(2)$, $b = 43.8747(10)$, $c = 18.6593(4)$ Å, $\beta = 94.4600(10)^\circ$, $V = 5958.7(2)$ Å³, $Z = 4$,

$D_x = 1.244$ g cm⁻³, $\mu = 4.166$ mm⁻¹. CCDC deposition number: 1580602.

3 | RESULTS AND DISCUSSIONS

3.1 | Crystal and molecular structures

The molecular structure along with crystallographic numbering scheme for the binuclear copper complex is shown in Figure 1. Although the structure is devoid of crystallographic symmetry, it has pseudo two fold symmetry with the axis bisecting the central C—C bond of the bridging bipy ligand and lying in the plane of defined by Cu1, Cu3, N1, and N31 atoms. The coordination geometry for the Cu1 atom is defined by N atoms of the chelating phen ligand, an N atom of one end of the bridging bipy ligand, an N atom of a terminally bound bipy ligand, an aqua-O atom and one O atom of the nitrate anion. The immediate environment of the Cu1 atom is

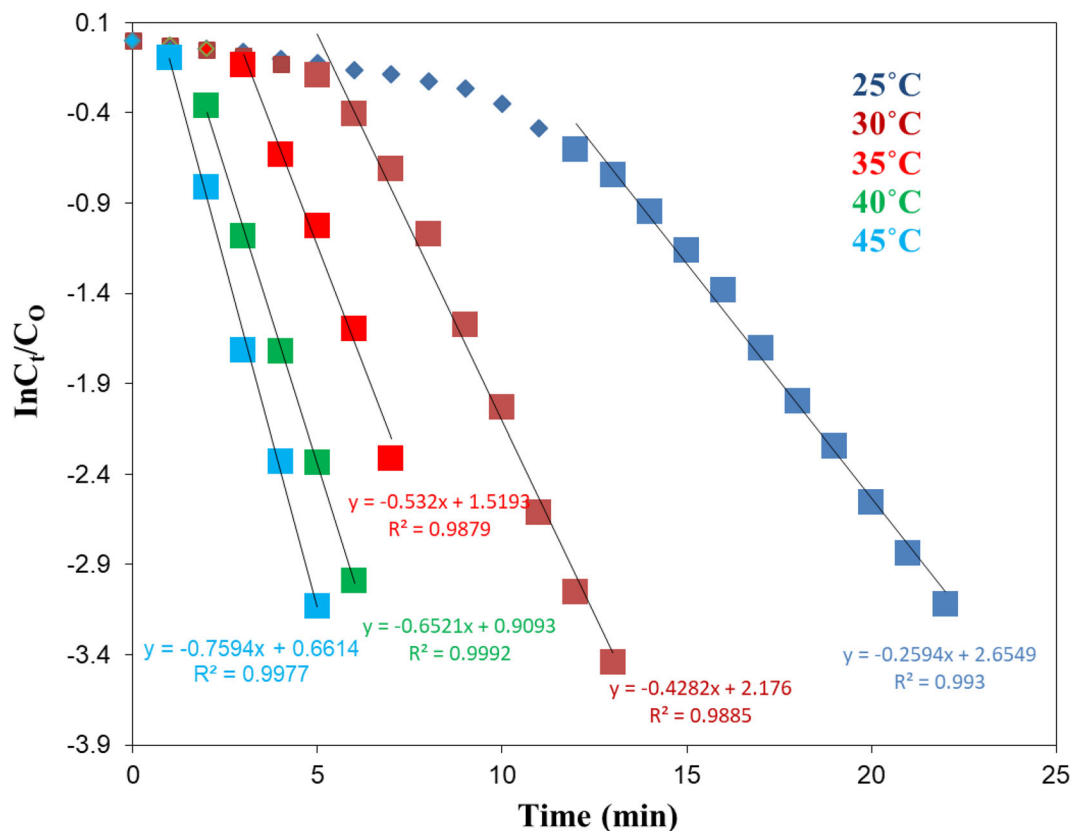


FIGURE 4 $\ln C_t/C_0$ versus time graph for *p*-nitrophenol (PNP) conversion to *p*-aminophenol (PAP) at different temperatures

defined by the N_4O_2 donor set and is best described as 5 + 1 as the Cu—O63 bond length is significantly longer than the other bonds as seen from the data collated in Table 1; an analogous coordination geometry is seen for the Cu3 atom. Nevertheless, the coordination geometry is based on an octahedron. There are a small number of literature precedents for the aforementioned structure. Thus, the $Cu_2(phen)_2(bipy)_3$ fragment has been observed in the structure of the copper(II) complex $[(L\text{-valinato-N,O})(bipy)(H_2O)Cu(bipy)Cu(L\text{-valinato-N,O})(bipy)(OH_2)](NO_3)_2 \cdot 2H_2O$ ^[44] but where the terminal bipy ligands have an antidisposition as opposed to *syn* in **1**; the Cu atoms have square pyramidal geometries with aqua ligands in the apical positions. An antidisposition is also found in the structure of $[(phen)(bipyH)(H_2O)Cu(bipy)Cu(phen)(bipyH)(OH_2)][Mo_{12}O_{40}P]_2 \cdot 2H_2O$ ^[45] that is, with protonated terminally bound bipy ligands, where the bulky counter ions cannot approach the copper centers resulting in square pyramidal geometries again with the aqua ligands in the apical positions. Of particular interest in the structure of **1** is the mode of supramolecular aggregation occurring in the crystal.

As anticipated, conventional hydrogen bonding plays a significant role in the molecular packing of **1** (Table S1). Thus, aqua—O—H \cdots O (nitrate) hydrogen bonds, involving

both pairs of independent aqua molecules and nitrate anions, leads to the formation of supramolecular chains along the *a*-axis. As viewed from Figure 2a, the chain is linear, and as both terminal bipy molecules are oriented to the same side, the topology is of a U-tube. The remaining aqua-H atoms form hydrogen bonds to the noncoordinating pyridyl-N atoms derived from two symmetry-related U-tubes, of opposite orientation, to generate layers in the *ac*-plane and, crucially, approximately square channels parallel to *a*-axis direction (Figure 2b). The channels have disparate edge lengths and the maximum dimensions of the face, based on the Cu \cdots Cu separations, are $8.8 \times 11.0 \times 12.0 \times 13.1$ Å. The layers stack along the *b*-axis with the primary connections between them being of the type phen—C—H \cdots O (nitrate) (Table S1). In this way, additional channels are formed, which is more symmetrical with each edge, again based on Cu \cdots Cu separations, being 10.7 Å (Figure 2c).

3.2 | Catalytic activity

The catalytic ability of **1** was evaluated for the PNP's reduction into PAP using $NaBH_4$, a prototype reaction. The reduction was followed readily by UV-vis

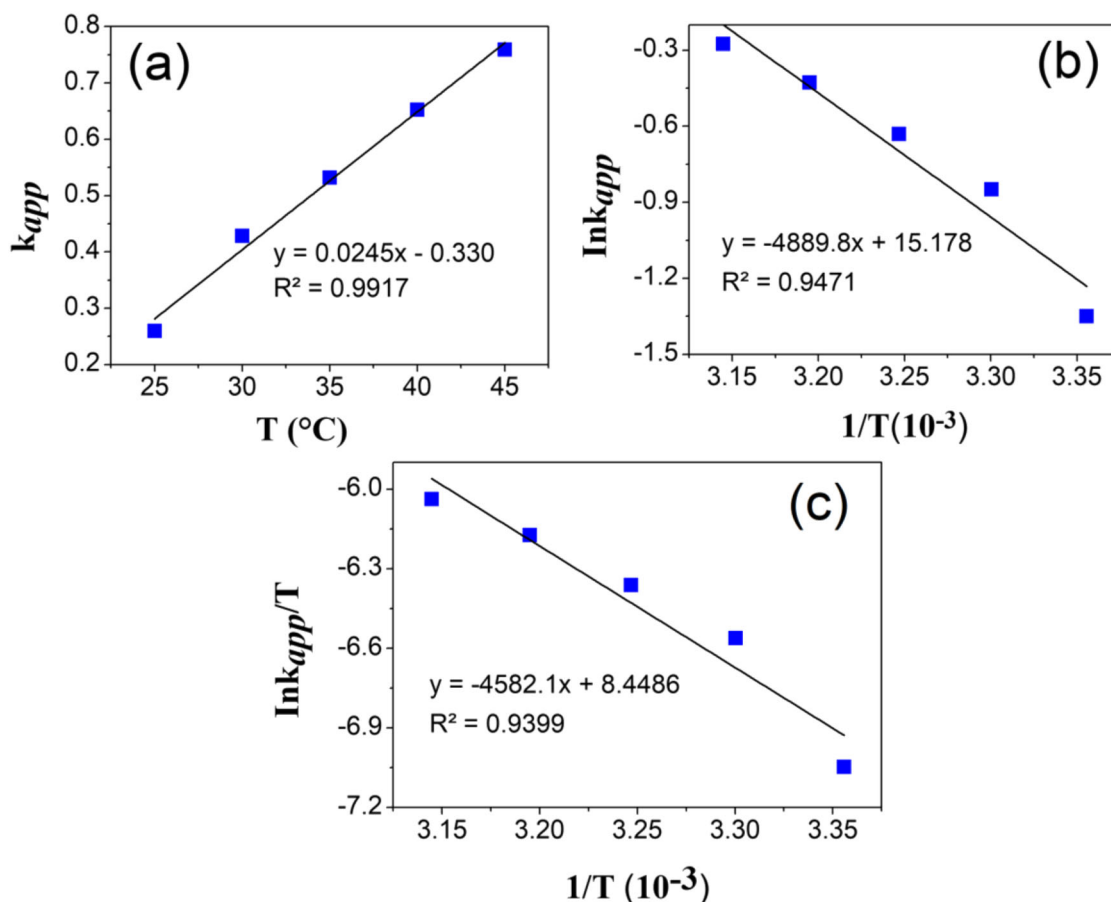


FIGURE 5 Plots of (a) K_{app} versus temperature, (b) $\ln k_{app}$ versus $1/T$, and (c) $\ln k_{app}/T$ versus $1/T$

spectroscopy as both reactant (PNP) and product (PAP) absorb in the UV-vis region at different λ_{max} values.^[46] Without a catalyst, the only obvious change noted was deepening of the yellow appearance of PNP upon the addition of NaBH_4 accompanied by a red shift (317–400 nm), signifying the formation of PNP ions (Figure S1). The absence of a peak pertinent to PAP, even after keeping the solution for several days, indicated that the reaction required a catalyst to proceed.^[47] However, in the presence of **1**, PNP to PAP conversion occurred after a few minutes as signified by the diminishing of

the peak of PNP (400 nm) and the emergence of a new peak for PAP at 290 nm^[48] (Figure 3a–e). In the induction period, the time required for the diffusion of reagents and catalyst $\ln C_t/C_o$ value remains unchanged. Excess NaBH_4 was used, and the linearity of $\ln C_t/C_o$ versus temperature relationship indicated pseudo-first-order kinetics.^[49] Afterward, the catalytic conversion of PNP to PAP was studied at five different temperatures (Figure 3a–e). The induction time decreases as does the reaction time, that is, from 22 (25°C) to 5 min (45°C). Furthermore, a threefold

TABLE 2 Kinetic parameters for the conversion of PNP to PAP

Temp (°C)	K_{app} (min^{-1})	E_a (kJ mol^{-1})	ΔH^\ddagger (kJ mol^{-1})	ΔS^\ddagger ($\text{J mol}^{-1} \text{K}^{-1}$)	TOF (min^{-1})
25	0.259	40.65	38.09	−197.51	0.0024
30	0.428	—	—	—	0.0040
35	0.532	—	—	—	0.0075
40	0.652	—	—	—	0.0087
45	0.759	—	—	—	0.010

Abbreviation: TOF, turn over frequency.

increase in the apparent rate constant was witnessed as the temperature rose from 25°C to 45°C (Figure 4). This correlated with an increase in the average kinetic energy of molecules at elevated temperature, which in turn increases the diffusion rate of the reactants. Hence, an increase in collision frequency and a fast diffusion rate triggered the conversion of reactants into products.^[50] The Arrhenius equation, that is, $\ln k = \ln A - E_a/RT$, was used to calculate E_a by plotting $\ln k$ versus $1/T$ gives a slope E_a/RT that corresponds E_a value of 40.65 kJ mol⁻¹.^[51] The kinetic parameters such as activation entropy (ΔS^\ddagger) and enthalpy (ΔH^\ddagger) were calculated using the Eyring equation, that is, $\ln k/T = \ln(k_b/h) + \Delta S^\ddagger/R - \Delta H^\ddagger/R (1/T)$,^[52] where T is the absolute temperature, k_b is the Boltzmann constant, h is the Planck constant, and R is the ideal gas constant. The plot of $\ln k_{app}/T$ versus $1/T$ gives a straight line with slope $-\Delta H^\ddagger/R$ (Figure 5) and intercept $(\ln(k_b/h) + \Delta S^\ddagger/R)$ from which $-\Delta H^\ddagger$ (38.09 kJ mol⁻¹) and ΔS^\ddagger (-197.51 J mol⁻¹ K⁻¹) can be calculated (Table 2). The positive ΔH^\ddagger value reflects the endothermic nature of the reduction process.

4 | CONCLUSIONS

Crystallography established **1** to contain well-defined channels, which, when evacuated, can accommodate guest species to facilitate the conversion of environmentally detrimental PNP to pharmaceutically useful PAP. It can be envisaged that the cationic form of the complex **1**, after ionization of NO₃⁻, has a high affinity for PNP and BH₄⁻ anions that are encapsulated in the pores to undergo the redox reaction. PNP to PAP conversion, which otherwise not possible in the absence of a suitable catalyst, completed within a few minutes in the presence of **1**. This study demonstrated that **1** with zeolite like channels can find applications as a reduction catalyst both on laboratory and industrial scales, and can catalyze reactions of environmental significance.

ACKNOWLEDGMENT

We acknowledge the financial support from the Higher Education Commission of Pakistan.

AUTHOR CONTRIBUTIONS

Abrar Ahmad: Investigation; methodology. **Syed Niaz Ali Shah:** Data curation; investigation; methodology. **Mehwish Arshad:** Investigation. **Francine Bélanger-Garipey:** Data curation; formal analysis; software. **Edward Tiekink:** Data curation; investigation; software. **Zia ur Rehman:** Conceptualization; funding acquisition; investigation; methodology; resources; supervision.

CONFLICT OF INTEREST

There is no conflict of interest.

DATA AVAILABILITY STATEMENT

The authors confirm that the data supporting the findings of this study are available within the article and its supplementary materials.

ORCID

Syed Niaz Ali Shah  <https://orcid.org/0000-0001-9902-857X>

Edward R.T. Tiekink  <https://orcid.org/0000-0003-1401-1520>

Zia ur Rehman  <https://orcid.org/0000-0002-1436-3131>

REFERENCES

- [1] F.-H. Lin, R.-A. Doong, *Appl. Catal., A* **2014**, *486*, 32.
- [2] J. Feng, L. Su, Y. Ma, C. Ren, Q. Guo, X. Chen, *Chem. Eng. J.* **2013**, *221*, 16.
- [3] P. K. Arora, A. Srivastava, V. P. Singh, *J. Hazard. Mater.* **2014**, *266*, 42.
- [4] Z. Dong, X. Le, C. Dong, W. Zhang, X. Li, J. Ma, *Appl. Catal. B.* **2015**, *162*, 372.
- [5] E. Marais, T. Nyokong, *J. Hazard. Mater.* **2008**, *152*, 293.
- [6] O. A. O'Connor, L. Young, *Environ. Toxicol. Chem.* **1989**, *8*, 853.
- [7] M. S. Dieckmann, K. A. Gray, *Water Res.* **1996**, *30*, 1169.
- [8] M. A. Oturan, J. Peiroten, P. Chartrin, A. J. Acher, *Environ. Sci. Technol.* **2000**, *34*, 3474.
- [9] N. Modirshahla, M. Behnajady, S. Mohammadi-Aghdam, *J. Hazard. Mater.* **2008**, *154*, 778.
- [10] P. Canizares, C. Saez, J. Lobato, M. Rodrigo, *Ind. Eng. Chem. Res.* **2004**, *43*, 1944.
- [11] S. Saha, A. Pal, S. Kundu, S. Basu, T. Pal, *Langmuir* **2009**, *26*, 2885.
- [12] Y.-C. Chang, D.-H. Chen, *J. Hazard. Mater.* **2009**, *165*, 664.
- [13] a) D. Huang, G. Yang, X. Feng, X. Lai, P. Zhao, *New J. Chem.* **2015**, *39*, 4685. b) P. Pachfule, S. Kandambeth, D. D. Diaz, R. Banerjee, *Chem. Commun.* **2014**, *50*, 3169. c) R. Fenger, E. Fertitta, H. Kirmse, A. Thünemann, K. Rademann, *Phys. Chem. Chem. Phys.* **2012**, *14*, 9343.
- [14] a) P. Zhang, C. Shao, Z. Zhang, M. Zhang, J. Mu, Z. Guo, Y. Liu, *Nanoscale* **2011**, *3*, 3357. b) Z. Wang, S. Zhai, B. Zhai, Z. Xiao, F. Zhang, Q. An, *New J. Chem.* **2014**, *38*, 3999. c) S. Xiao, W. Xu, H. Ma, X. Fang, *RSC Adv.* **2012**, *2*, 319.
- [15] a) C. Deraedt, L. Salmon, D. Astruc, *Adv. Synth. Catal.* **2014**, *356*, 2525. b) Z. Wang, C. Xu, G. Gao, X. Li, *RSC Adv.* **2014**, *4*, 13644. c) X. Gu, W. Qi, X. Xu, Z. Sun, L. Zhang, W. Liu, X. Pan, D. Su, *Nanoscale* **2014**, *6*, 6609.
- [16] a) A. K. Patra, A. Dutta, A. Bhaumik, *Cat. Com.* **2010**, *11*, 651. b) P. Deka, R. C. Deka, P. Bharali, *New J. Chem.* **2014**, *38*, 1789. c) P. Zhang, Y. Sui, G. Xiao, Y. Wang, C. Wang, B. Liu, G. Zou, B. Zou, *J. Mater. Chem. A* **2013**, *1*, 1632.
- [17] A. Goyal, S. Bansal, S. Singhal, *Int. J. Hydrogen Energy* **2014**, *39*, 4895.
- [18] H. Zhang, S. Gao, N. Shang, C. Wang, Z. Wang, *RSC Adv.* **2014**, *4*, 31328.

- [19] J. Li, L. Zhang, X. Liu, N. Shang, S. Gao, C. Feng, C. Wang, Z. Wang, *New J. Chem.* **2018**, *42*, 9684.
- [20] H. Zhang, Y. Zhao, W. Liu, S. Gao, N. Shang, C. Wang, Z. Wang, *Cat. Com.* **2015**, *59*, 161.
- [21] B. Hoskins, R. Robson, *J. Am. Chem. Soc.* **1990**, *112*, 1546.
- [22] P. Z. Moghadam, A. Li, S. B. Wiggin, A. Tao, A. G. Maloney, P. A. Wood, S. C. Ward, D. Fairen-Jimenez, *Chem. Mater.* **2017**, *29*, 2618.
- [23] a) B. Moulton, M. J. Zaworotko, *Chem. Rev.* **2001**, *101*, 1629. b) A. J. Howarth, Y. Liu, P. Li, Z. Li, T. C. Wang, J. T. Hupp, O. K. Farha, *Nat. Rev. Mater.* **2016**, *1*, 15018.
- [24] a) K. T. Mahmudov, M. N. Kopylovich, M. F. C. G. da Silva, A. J. Pombeiro, *Coord. Chem. Rev.* **2017**, *345*, 54. b) E. R. Tiekink, *Coord. Chem. Rev.* **2017**, *345*, 209.
- [25] a) J. Reedijk, *Chem. Soc. Rev.* **2013**, *42*, 1776. b) N. Adarsh, P. Dastidar, *Chem. Soc. Rev.* **2012**, *41*, 3039.
- [26] a) K. Rissanen, *CrystEngComm* **2008**, *10*, 1107. b) B. Li, S.-Q. Zang, L.-Y. Wang, T. C. Mak, *Coord. Chem. Rev.* **2016**, *308*, 1.
- [27] a) S. J. Garibay, J. R. Stork, S. M. Cohen, *Prog. Inorg. Chem.* **2009**, *56*, 335. b) G. Kumar, R. Gupta, *Chem. Soc. Rev.* **2013**, *42*, 9403.
- [28] F. Chen, Y. Chen, H. Cao, Q. Xu, L. Yu, *J. Org. Chem.* **2018**, *83*, 14158.
- [29] Y. Chen, Q. Zhang, X. Jing, J. Han, L. Yu, *Mater. Lett.* **2019**, *242*, 170.
- [30] F. Xin, Y. Rong, W. Fang, Z. Xu, X. Qing, Y. Lei, *Chinese J. Org. Chem.* **2018**, *38*, 2736.
- [31] D. Soriano del Amo, W. Wang, H. Jiang, C. Besanceney, A. C. Yan, M. Levy, Y. Liu, F. L. Marlow, P. Wu, *J. Am. Chem. Soc.* **2010**, *132*, 16893.
- [32] A. P. Ingle, N. Duran, M. Rai, *Appl. Microbiol. Biotechnol.* **2014**, *98*, 1001.
- [33] a) A. Zanon, F. Verpoort, *Coord. Chem. Rev.* **2017**, *353*, 201. b) K. Vellingiri, L. Philip, K.-H. Kim, *Coord. Chem. Rev.* **2017**, *353*, 159. c) Z. Hu, D. Zhao, *CrystEngComm* **2017**, *19*, 4066. d) Q. Yang, Q. Xu, H.-L. Jiang, *Chem. Soc. Rev.* **2017**, *46*, 4774. e) L. Zhu, X.-Q. Liu, H.-L. Jiang, L.-B. Sun, *Chem. Rev.* **2017**, *117*, 8129. f) C. Pagis, M. Ferbinteanu, G. Rothenberg, S. Tanase, *ACS Catal.* **2016**, *6*, 6063.
- [34] S. Oh, S. Lee, M. Oh, *ACS Appl. Mater. Interfaces* **2020**, *12*, 18625.
- [35] M. A. Ahsan, E. Deemer, O. Fernandez-Delgado, H. Wang, M. L. Curry, A. A. El-Gendy, J. C. Noveron, *Cat. Com.* **2019**, *130*, 105753.
- [36] M. Iqbal, S. Ali, Z.-U. Rehman, N. Muhammad, M. Sohail, V. Pandarinathan, *J. Coord. Chem.* **2014**, *67*, 1731.
- [37] V. Saint, Madison, WI, USA, **2014**.
- [38] S. Version, *Acta Crystallogr., Sect. A: Found. Crystallogr.* **2008**, A64.
- [39] G. M. Sheldrick, *Acta Crystallogr., Sect. C: Struct. Chem.* **2015**, *71*, 3.
- [40] O. V. Dolomanov, A. J. Blake, N. R. Champness, M. Schröder, *J. Appl. Crystallogr.* **2003**, *36*, 1283.
- [41] P. Squeeze, *Acta Crystallogr., Sect. C: Struct. Chem.* **2015**, *71*, 9.
- [42] L. J. Farrugia, *J. Appl. Crystallogr.* **2012**, *45*, 849.
- [43] C. Impact, Crystal Impact GbR, Bonn, Germany **2006**.
- [44] B.-Y. Lou, M.-C. Hong, *Acta Crystallogr., Sect. E: Struct. Rep. Online* **2008**, 64.
- [45] D.-D. Yang, B. Mu, L. Lv, R.-D. Huang, *J. Coord. Chem.* **2015**, *68*, 752.
- [46] N. Sahiner, S. Butun, O. Ozay, B. Dibek, *J. Colloid Interface Sci.* **2012**, *373*, 122.
- [47] M. Nasrollahzadeh, S. M. Sajadi, A. Rostami-Vartooni, M. Bagherzadeh, *J. Colloid Interface Sci.* **2015**, *448*, 106.
- [48] K. Kuroda, T. Ishida, M. Haruta, *J. Mol. Catal. A: Chem.* **2009**, *298*, 7.
- [49] a) S. ur Rehman, M. Siddiq, H. Al-Lohedan, N. Sahiner, *Chem. Eng. J.* **2015**, *265*, 201. b) X. Le, Z. Dong, W. Zhang, X. Li, J. Ma, *J. Mol. Catal. A: Chem.* **2014**, *395*, 58.
- [50] S. Wu, J. Dzubiella, J. Kaiser, M. Drechsler, X. Guo, M. Ballauff, Y. Lu, *Angew. Chem., Int. Ed.* **2012**, *51*, 2229.
- [51] M. Ajmal, Z. H. Farooqi, M. Siddiq, *Korean J. Chem. Eng.* **2013**, *30*, 2030.
- [52] a) N. Sahiner, N. Karakoyun, D. Alpaslan, N. Aktas, *Int. J. Polym. Mater. Polym. Biomater.* **2013**, *62*, 590. b) S. Butun, N. Sahiner, *Polymer* **2011**, *52*, 4834.

SUPPORTING INFORMATION

Additional supporting information may be found online in the Supporting Information section at the end of this article.

How to cite this article: Ahmad A, Shah SNA, Arshad M, Bélanger-Gariepy F, Tiekink ERT, ur Rehman Z. A copper diimine-based honeycomb-like porous network as an efficient reduction catalyst. *Appl Organomet Chem.* 2020;e6065. <https://doi.org/10.1002/aoc.6065>